Available online at www.sciencedirect.com
SCIENCE DIRECT®
Sensors and Actuators B 97 (2004) 409–414
SENSORS AND ACTUATORS B CHEMICAL
www.elsevier.com/locate/snb

Near-infrared surface plasmon resonance sensing on a silicon platform

Sergiy Patskovsky [a,*], Andrei V. Kabashin [a], Michel Meunier [a], John H.T. Luong [b]

[a] *Laser Processing Laboratory, Department of Engineering Physics, Ecole Polytechnique de Montreal, Case Postale 6079, Succ. Centre-ville, Montreal, Que., Canada, H3C 3A7*

[b] *Biotechnology Research Institute, National Research Council Canada, Montreal, Que., Canada, H4P 2R2*

Received 21 January 2003; received in revised form 14 September 2003; accepted 22 September 2003

Abstract

A novel surface plasmon resonance (SPR) sensing configuration equipped with a silicon coupling prism is described. Theoretical results and experimental data are obtained to establish essential conditions of SPR excitation using infrared light in the Kretschmann–Raether geometry with a thin gold layer as the supporting metal. We also compare sensitivities of different angular and spectral interrogation Si-based schemes in models of bio- and chemical sensing. Possibilities for the miniaturization of SPR sensors using the proposed Si-based configuration are discussed.

Keywords: Surface plasmon resonance; Miniaturization; Silicon prism; Infrared

1. Introduction

With the impressive progress in the development of optical transduction biodetection methods over the last decade, surface plasmon resonance (SPR) has become a widely used laboratory tool to study biological recognition and binding events [1,2]. SPR sensor systems are usually implemented in the Kretschmann–Raether prism geometry [3], as shown in Fig. 1, with the use of visible light and a glass prism. However, the conventional dielectric glass-based SPR technology imposes severe limitations on miniaturization of sensing schemes. Consequently, SPR sensors are mainly designed as bulky laboratory systems with the use of ultra-precision stages and high-resolution equipment [4,5].

We have recently examined SPR dispersion characteristics in near-infrared range (1100–2300 nm) of different prism materials, including dielectrics (BK7 and SF11 glasses) and semiconductors (silicon), and showed a possibility for the reproduction of SPR effect on a purely silicon platform [6]. We reason that the use of such a silicon platform gives a promise for the miniaturization of the SPR technique and the creation of inexpensive and portable micro SPR sensors for the field applications. This expectation is based on the advanced development of the methods for silicon microfabrication that can significantly facilitate the miniaturization and integration of the sensor transducer, emitter, detector, and processing electronics on a single Si-based chip [7]. In addition, Si-based technology makes possible the formation of microfluidic systems and multi-channel arrays. However, the implementation of the miniaturized SPR schemes requires a detailed knowledge of parameters of the SPR production for the silicon platform as a prerequisite, because silicon dispersion characteristics significantly differ from those of the glasses [6].

In this paper, we present a detailed study of conditions of SPR production and sensing characteristics of the silicon platform. Schemes with both angular and spectral interrogation are considered in conditions of bio- and chemical sensing.

2. Theoretical framework

SPR consists in a resonance transfer of pumping light energy to a surface plasmon mode, coupled to collective oscillations of electrons in a metal [3]. As existing at a metal/dielectric interface, the plasmons can be represented by the dispersion relation for two homogeneous semi-infinite media:

$$k_{SP_0} = \frac{\omega}{c}\left(\frac{\varepsilon_m(\omega)\varepsilon_s(\omega)}{\varepsilon_m(\omega)+\varepsilon_s(\omega)}\right)^{1/2} \quad (1)$$

* Corresponding author. Tel.: +1-514-340-4711x2995; fax: +1-514-340-3218.
E-mail address: psv@canada.com (S. Patskovsky).

0925-4005/$ – see front matter © 2003 Elsevier B.V. All rights reserved.
doi:10.1016/j.snb.2003.09.023

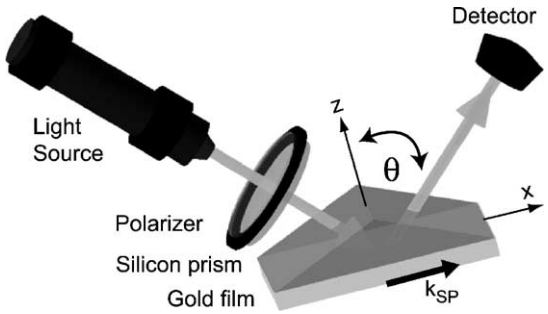

Fig. 1. Schematic of the SPR system with a silicon sensing prism used in the experiment.

where $k_{SP_0} = k'_{SP_0} + i\Gamma_i$ is a wave vector of surface plasmons (Γ_i is the intrinsic loss term), ε_m and ε_s, are dielectric constants of the metal and dielectric sample media, ω the wave frequency, and c is the velocity of light. SPR is generally produced in the Kretschmann–Raether prism arrangement scheme [3], in which p-polarized visible light is directed through a prism with a relatively high refractive index n_p and then reflected from the gold film deposited on the prism surface (Fig. 1). The conversion of the pumping wave to the surface plasmon wave is achieved by matching the projection of the wave number of the incident beam on the surface k_x to the surface plasmon wave number k_{SP} at a specific combination of the pumping frequency ω and the angle of incidence θ_{SPR}:

$$n_p \frac{\omega}{c} \sin\theta_{SPR} = k_{SP} \tag{2}$$

The excitation of surface plasmon wave leads to the appearance of the dip in the angular (spectral) dependence, depending upon the reflected light intensity. The dip position is extremely sensitive to the dielectric constant of the adjacent sample medium ε_s, within a thin layer near the interface. This enables to study bio- and chemical interactions in thin films on gold, resulting in a refractive index (layer thickness) change [1,2]. To characterize conditions of SPR production, one should also take into consideration the system perturbation due to the presence of the prism and the finiteness of layers, which lead to certain change of the wave number of surface plasmons k_{SP} (Eq. (1)). In this study, this perturbation is taken into account by incorporating the loss term wave number $k_r = k'_r + i\Gamma_r$ (Γ_r is a re-radiative loss term). As a result, the complex wave vector of the surface plasmons can be expressed as [3,8,9]

$$k_{SP} = k_{SP_0} + k_r \tag{3}$$

where k_{SP_0} is the wave number in the absence of the sensing prism (Eq. (1)). A solution for Eq. (2) through the pumping wavelength λ and θ_{SPR} enables the determination of the SPR conditions. The reflectivity in the immediate vicinity of the resonance R and the width of the SPR dip W_k can be expressed as [8]:

$$R = 1 - \frac{4\Gamma_i\Gamma_r}{(k_x - k'_{SP})^2 + (\Gamma_i + \Gamma_r)^2};$$
$$W_k = \frac{2(\Gamma_i + \Gamma_r)}{n_p(\omega/c)\cos\theta_{SPR}} \tag{5}$$

In this study, we consider air and water as two typical sample media. The dispersion relation for water was taken from Harvey et al. [10], with a correction factor due to weak water absorption taken from the data of Kou et al. [11]. Dispersion properties of gold in visible and IR light were taken from the data of Innes and Sambles [12] and Johansen et al. [13]. The gold film thickness was optimized using equations from Kurihara and Suzuki [8]. The optical constants for silicon were obtained from the approximation of experimental dependencies reported by Herzinger et al. [14].

3. Experimental

The SPR coupling system consisted of a silicon prism, a gold film, and a flow cell, as shown in Fig. 1. The flow cell was empty or filled with deionized water, depending on whether the sensing sample medium was air or liquid. The gold film was deposited on the prism or, in some cases, on a 0.5 mm thick silicon wafer, which was then placed in intimate contact with the silicon prism. Two silicon prisms (p-type, $\rho > 20\,\Omega$ cm, Almaz Optics, West Berlin, NJ) with a base angle of $\alpha = 16.6^\circ$ and 22.4°, respectively, were custom made for our study. Such prisms conditioned the incidence of the laser beam onto the silicon/gold interface at angles close to θ_{SPR} obtained from theoretical calculations. Our tests showed that even prisms from standard doped silicon were transparent enough in the near-IR 1100–1700 nm range and the use of optical elements from expensive FZ silicon with highest resistance and lowest light losses was unnecessary.

The gold layer thickness (40 nm) was selected to provide relatively low reflected light intensity with SPR sensing in the range of 1100–1700 nm according our optimizations in [6]. The SPR coupling system (with or without the flow cell) was placed onto a rotary block of a variable angle spectroscopic ellipsometer (Woollam VASE® ellipsometer, J.A. Woollam, Lincoln, NE) to allow for a very fine variation of the angular prism position with respect to the optical path of the ellipsometer. The system was illuminated by monochromatic p-polarized light with variable wavelengths, obtained by passing white light through the monochromator. The light reflected from the coupling system was analyzed by two detectors, whose characteristics determined the dynamic range of the spectral measurement from 193 to 1700 nm. The experiments were performed with a configuration of a fixed wavelength (angular interrogation) or incident angle (spectral interrogation). The precision of angular and spectral measurements was 0.005° and 0.1 nm, respectively.

4. Results and discussion

Fig. 2 presents typical angular reflectivity curves from the theory (broken line) and experimental data (solid line) for the gaseous (a) and aqueous (b) sample media. The presented curves correspond to different wavelengths of the pumping light. As presented by the experimental curves, the angles were related to the prism/gold interface, while a slight light refraction at the entrance to the prism was taken into account as a correction coefficient. Essentially, the main trend of the theory was well confirmed by the experimental data and the calculated positions of reflectivity minima well correlated with the measured ones.

The SPR effect on the silicon prism was achieved at relatively narrow ranges of incident angles θ_{SPR} of 16.5°–16.8° and 22.35°–22.45° for gaseous and aqueous sample media, respectively (Fig. 2). These values were much lower in comparison with the glass prism case [6,15], due to a relatively high refractive index of silicon ($n \sim 3.45$–3.6 in the IR range [14]) in comparison with that of dielectrics and the sample media. It is noteworthy that the experimental reflectivity curves were slightly broader as compared to the theoretical ones. In particular, for $\lambda = 1200$ nm the experimental values of full width at half maximum (FWHM) were 0.12° for gaseous and 0.18° for aqueous sample media, whereas the relevant calculated values did not exceed 0.066° and 0.16°, respectively. We recently showed that the relative broadness of the experimental curves W_k is mainly related to a certain roughness of the deposited gold films and a non-uniformity of the film thickness [6]. The values of the curve widths for the silicon platform were at least two-fold smaller than in the glass prism case [6]. This agrees with Eq. (5), showing that the width W_k of the reflectivity curve is inversely proportional to the prism refractive index. As shown in Fig. 2, the position of the reflectivity minimum was dependent upon the wavelength of pumping light. For each wavelength, an appropriate angle of incidence could be selected to provide resonant conditions.

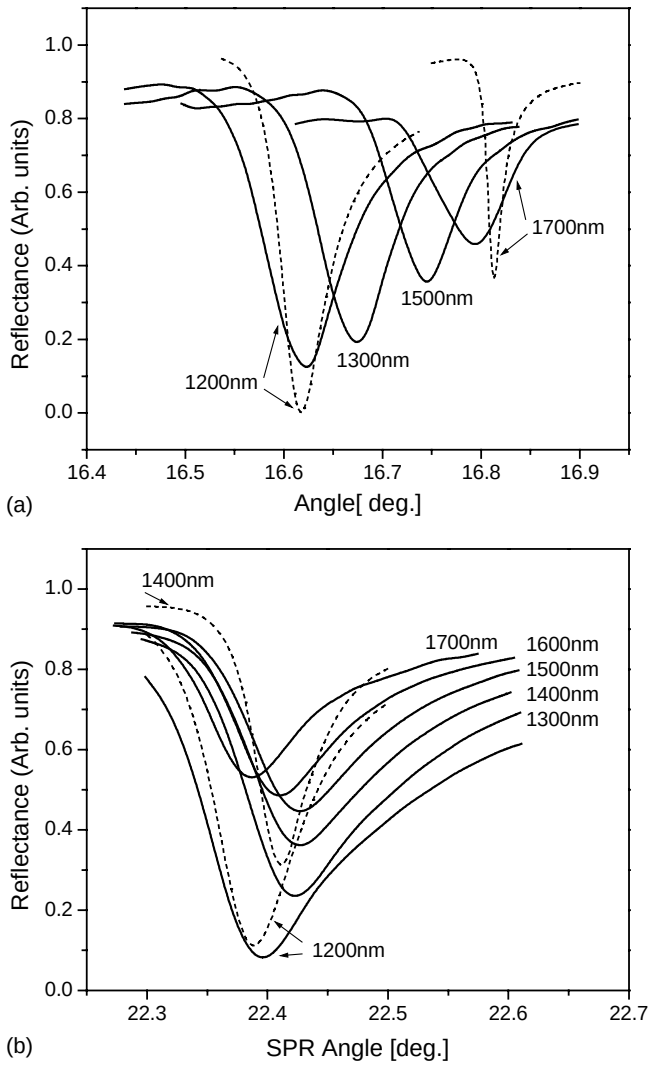

Fig. 2. Typical angular reflectivity curves for the silicon prism in the configuration of gaseous (a) and aqueous (b) sample media. The broken and solid lines present the calculated and experimental data, respectively.

Similar SPR-related reflectivity minima were observed in the spectral dependence of the reflectivity when the angle of incidence was kept constant (Fig. 3). In this case, the position of the spectral minimum was very sensitive to the angle of incidence. As an example, in the gaseous medium (Fig. 3a), only a slight decrease of the incident angle from 16.8° to 16.5° led to a considerable shift of the reflectivity minimum from 1700 to 1100 nm. Another interesting feature was the appearance of two reflectivity minima under sensing with aqueous sample medium, as shown in Fig. 3b. Such a feature was apparently connected to particular dispersion properties of silicon and water in the IR range [6]. Note that sensing with aqueous medium was accompanied by a larger discrepancy between experimental and theoretical results (Fig. 3b). This discrepancy could be minimized by a further optimization of the gold layer thickness and a more precise angle setting during the experiment.

The data for the SPR minimum position collected from the angular and spectral reflectivity curves are summarized in Fig. 4, which describes the resonant conditions for a simultaneous variation in the wavelength and the angle of incidence. The SPR minimum angle and wavelength can be generated from these plots by taking a cut parallel to the *Y* or *X*-axis. As illustrated in this figure, in the air sensing medium, the increase of wavelength was accompanied by an increase in the resonant angle. This behavior was completely opposite to the conventional case of the glass prism used for SPR sensors in the visible and NIR [15]. In aqueous medium, the behavior of SPR dispersion curves became more complicated and intriguing (Fig. 4). The resonant angle initially increased with an increase in the wavelength and reached a maximum value at $\lambda = 1400$ nm and then decreased with a further increase in λ. As a result, for resonant angles above 22.35° spectral dependences were characterized by the simultaneous presence of two dips, as illustrated in Fig. 3b. Note that our experiments with the aqueous sample medium

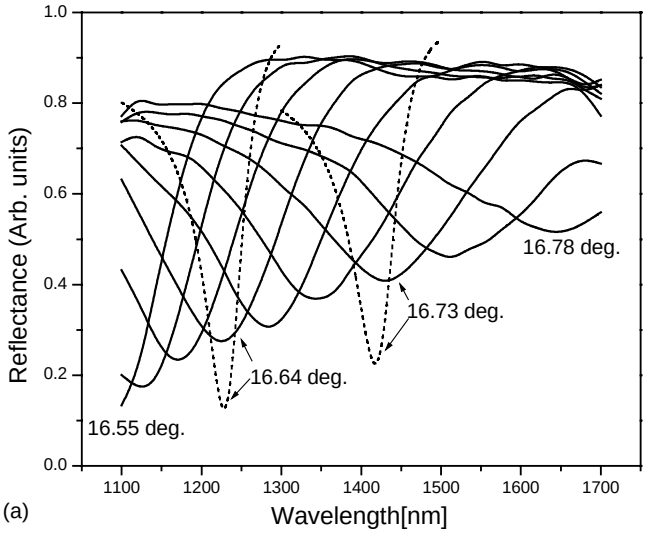

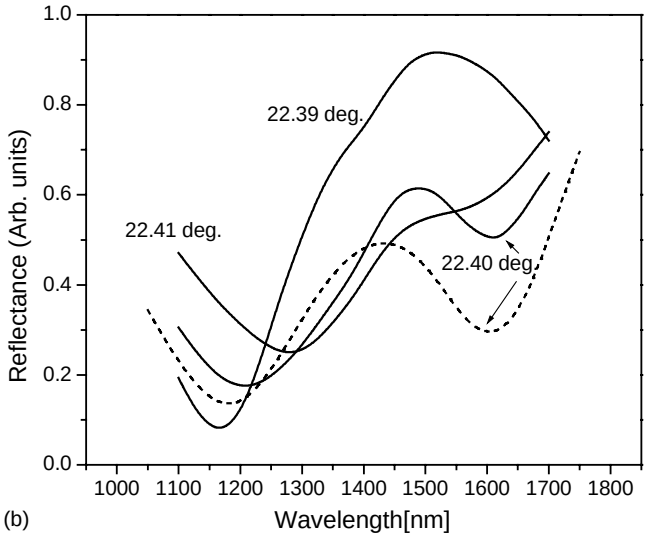

Fig. 3. Typical spectral reflectivity curves for the silicon prism in the configuration of gaseous (a) and aqueous (b) sample media. The broken and solid lines present the calculated and experimental data, respectively.

did not reveal any features in 1400–1450 nm range, where water has a slight anomalous dispersion. This dispersion was probably not visible in the spectral curves due to their relative broadness. With the angular interrogation, we simply avoided the fixation of the pumping wavelength in this range.

One of the most important parameters of SPR sensing is the response sensitivity. We consider the "absolute" bulk sensitivity that represents a simple angular or spectral shift of the SPR dip due to a change in the refractive index n_s. In the angular interrogation scheme, the position of the resonant angle of incidence θ_{SPR} is recorded, while the wavelength λ is kept constant. As shown in Fig. 5, in Si-based schemes the resonant angle θ_{SPR} shifts to larger values with an increase in the refractive index that is similar to the glass-based prism case [13]. In typical biosensing conditions with refractive index variations between 1.32 and 1.4, the range of angle variations does not exceed 2°, which is, however, sufficient to efficiently record the course of biological interactions. Since SPR minima are relatively narrow in the case of the silicon platform, one can measure the dip position with higher precision, and thus improve the resultant detection sensitivity (for a complete description of such systems, many authors use the so-called intrinsic sensitivity, corresponding to the shift of the SPR dip divided by its width for a given change of the refractive index [13]). Another important advantage of the Si-based scheme is a possibility of measurements in a wide dynamic range due to a relatively high refractive index of silicon. This extends the application area of the SPR technique to a characterization of thin solid or polymer films with relatively high refractive indices.

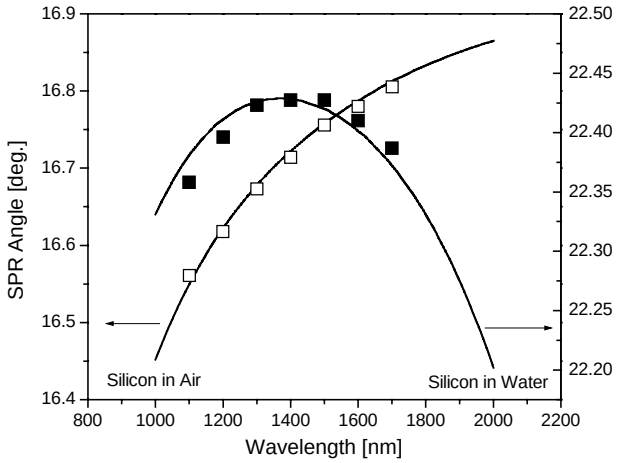

Fig. 4. SPR dispersion curves for in Si-based configurations with gaseous and aqueous sample media. The symbols present the experimental data, while the curves depict to the results of calculations.

In contrast, in the spectral interrogation configuration the response of the Si-based system appears to be opposite to

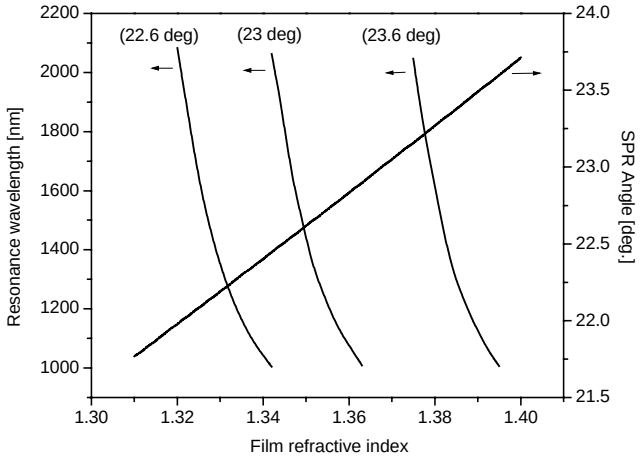

Fig. 5. Calculated angular and spectral sensing responses of the system to a change in the refractive index of the sample medium. The angular dependencies were obtained for the fixed pumping wavelength $\lambda = 1200$ nm. The spectral dependencies were obtained for several fixed angles of incidence.

the trend observed with glass. Indeed, for silicon wavelength λ_{SPR} decreased with an increase in the refractive index whereas this wavelength increased in the case of glass [6,13]. With a fixed angle θ, it was plausible to perform refractive index measurements over a relatively small range Δn_s, between 1.32 and 1.38 as illustrated in Fig. 5. Another range of Δn_s could be examined by changing the initial position of the angle of incidence. Using such angle adjustment, one may perform refractive index measurements in the same dynamic range as for the angular interrogation scheme. It is interesting to note that the bulk spectral sensitivity decreases when the wavelength decreases (Fig. 5). As we also showed in [6], a further decrease of the wavelength down to the visible range leads to an even larger drop in spectral sensitivity for glass-based schemes. Therefore, near-IR Si-based schemes operate in conditions of maximal spectral response.

In real chemical and biological sensing experiment, the bulk refractive index of the adjacent gaseous ($n_s \sim 1$) or aqueous ($n_s \sim 1.33$) medium is almost constant, while the thickness of the thin film on gold increases as a result of a selective binding or recognition event. In the calculations, we simulated the chemical and biological sensing processes by using model layers with $n_{film} = 1.1$ and 1.34–1.46, respectively. Such refractive index values are consistent with typical layers, which are used in chemical and biological sensing [1]. Fig. 6 shows the calculated relative change of the resonant angle $\Delta\theta_{SPR}$ as a function of Δd in the chemical sensing model. The response sensitivity depends on the thickness of the model film with a maximum of sensitivity between 150 and 400 nm. Nevertheless, the probe depth of the near-IR Si-based scheme can exceed 1.5 μm, which is much larger than in the case of visible light (200–300 nm) [4]. Similar results for maximum sensitivity and the probe depth up to 1.5–2 μm were obtained in the biosensing simulation model. Therefore, SPR schemes with IR light should be more efficient for remote sensing applications. From our perspective, this phenomenon might be used to monitor the sensing event far from the gold surface and/or to detect interactions of large objects with their receptors immobilized on the gold surface. Deadly viruses and bacteria are two important examples of such bio-objects, which cannot be detected by current visible-based SPR schemes.

It should be noted that sensing with aqueous sample medium was characterized by the presence of two minima in the spectral dependence at $\theta > 22.35^\circ$ (Fig. 3b) and the appearance of positive (at $\lambda < 1400$ nm) and negative ($\lambda > 1400$ nm) slopes in the SPR dispersion curve (Fig. 4). In the biosensing simulation, the increase of the thickness of the model film with $n_{film} = 1.4$ leads to a modification of the SPR dispersion curve, as shown in Fig. 7a. However, the polarity of sensing response appears to be opposite for

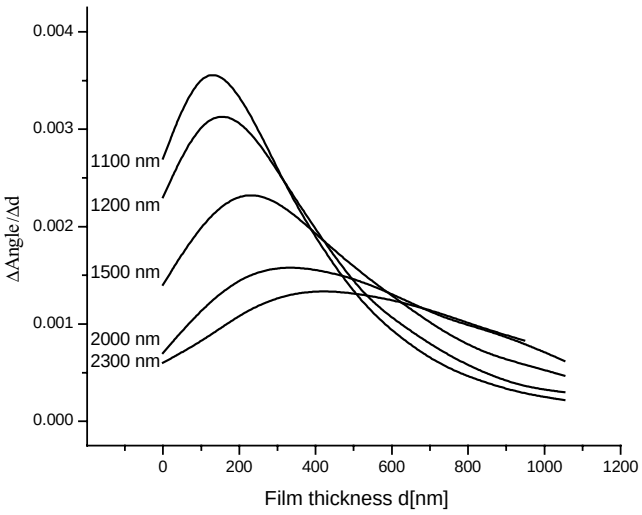

Fig. 6. Calculated angular response of the gas sensing system to the increase of the thickness (d) of a model dielectric layer with $n_{film} = 1.1$.

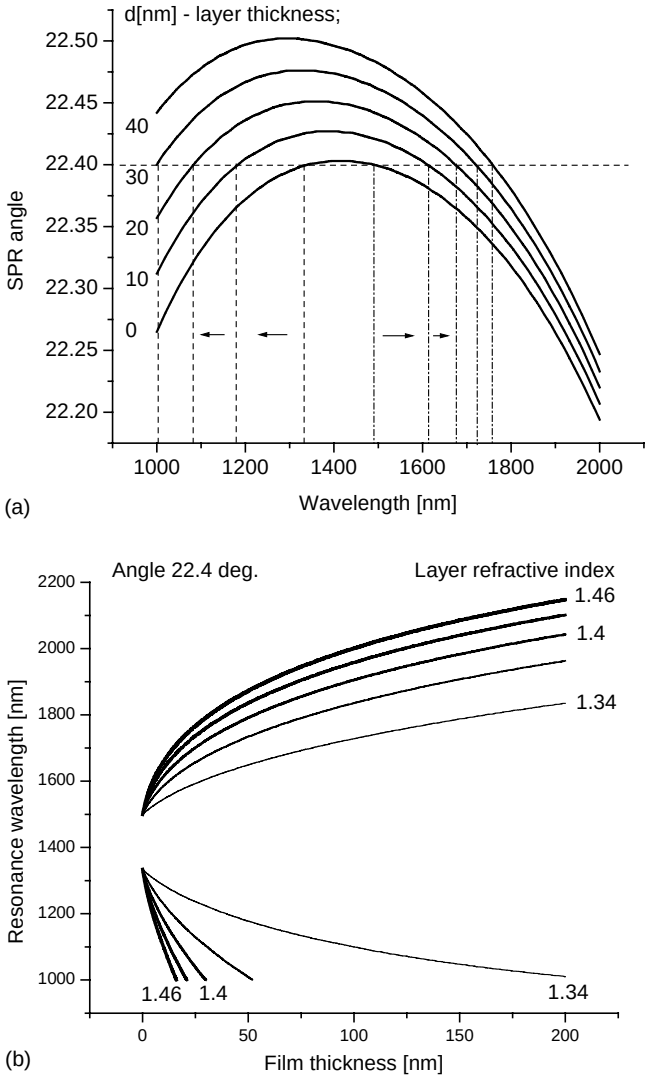

Fig. 7. (a) SPR dispersion curves in Si-based biosensing system for different thicknesses (d) of a model dielectric layer ($n_{film} = 1.4$). (b) The corresponding spectral response of two SPR minima to the layer thickness increase.

the two minima. Indeed, the thickness increase leads to a blue shift of the resonant wavelength λ_{SPR} at $\lambda < 1400$ nm and its red shift at $\lambda > 1400$ nm (Fig. 7b). In other words, the distance between two dips become wider as the thickness of the sensing layer increases. We reason that the data collected from positions of two minima can be used as two independent channels for a single sensing film under investigation. This phenomenon, granted by particular dispersion characteristics of silicon, could help to control simultaneously both the refractive index and the thickness of the biological film that is generally impossible in conventional glass-based SPR configuration [4,5].

We believe that the implementation of the SPR sensor on a silicon platform will enable to take advantage of methods for silicon microfabrication in order to facilitate the miniaturization and integration of a sensor device. In contrast to the conventional glass-based SPR platform, Si-based technology widespread application of SPR technology from expensive and cumbersome stationary laboratory systems to low-cost and portable microsensors with a simplified sensing parameter (e.g., in terms of yes/no) and design. In particular, these sensors can be used for the field sensing (e.g., for the detection of dangerous toxic agents with the use of biological substances immobilized on detachable slides) or as a part of micro total analysis system (μTAS).

5. Conclusion

Conditions and properties of SPR production in the Kretschmann–Raether geometry with the use of a silicon prism-based platform are studied. SPR characteristics for this platform can be significantly different compared to conventional glass-based schemes due to a difference of material dispersion properties. We also tested various sensing schemes in models of bio- and chemical sensing and discussed possibilities for the miniaturization and integration of SPR biosensors, using Si-based microfabrication methods.

Acknowledgements

The authors thank professor Ludvik Martinu of the Department of Engineering Physics, Ecole Polytechnique de Montreal for assistance with experimental facilities. We also acknowledge the financial contribution from the Natural Science and Engineering Research Council of Canada.

References

[1] P. Schuck, Use of surface plasmon resonance to probe the equilibrium and dynamic aspects of interactions between biological macromolecules, Annu. Rev. Biophys. Biomol. Struct. 26 (1997) 541–566.
[2] P.B. Garland, Optical evanescent wave methods for the study of biomolecular interactions, Q. Rev. Biophys. 29 (1996) 91–117.
[3] E. Kretschmann, H. Raether, Radiative decay of non-radiative surface plasmons excited by light, Z. Naturforsch. A 23 (1968) 2135–2136.
[4] B. Liedberg, C. Nylander, I. Lundstrom, Biosensing with surface plasmon resonance—how it all started, Biosens. Bioelectron. 10 (1995) i–ix.
[5] J.L. Melendez, R. Carr, D.U. Bartholomew, K.A. Kukanskis, J. Elkind, S.S. Yee, C.E. Furlong, R.G. Woodbury, A commercial solution for surface plasmon sensing, Sens. Actuators B 35 (1996) 212–216.
[6] S. Patskovsky, A.V. Kabashin, M. Meunier, J.H.T. Luong, Properties and sensing characteristics of surface plasmon resonance in infrared light, JOSA A 20 (2003) 1644–1650.
[7] M.J. Madou, Fundamentals of Microfabrication, CRC Press, New York, 1997.
[8] K. Kurihara, K. Suzuki, Theoretical understanding of an absorption-based surface plasmon resonance sensor based on Kretchmann's theory, Anal. Chem. 74 (2002) 666–671.
[9] E.M. Yeatman, Resolution and sensitivity in surface plasmon microscopy and sensing, Biosens. Bioelectron. 11 (1996) 635–649.
[10] A.H. Harvey, J.S. Gallagher, J.M.H. Levelt-Sengers, Revised formulation for the refractive index of water and steam as a function of wavelength, temperature and density, J. Phys. Chem. Ref. Data 27 (1968) 761–774.
[11] L. Kou, D. Labrie, P. Chylek, Refractive indices of water and ice in the 0.65–2.5 mm spectral range, Appl. Opt. 32 (1993) 3531–3540.
[12] R.A. Innes, J.R. Sambles, Optical characterisation of gold using surface plasmon-polaritons, J. Phys. F 17 (1987) 277–287.
[13] K. Johansen, H. Arwin, I. Lundström, B. Liedberg, Imaging surface plasmon resonance sensor based on multiple wavelengths: sensitivity considerations, Rev. Sci. Instrum. 71 (2000) 3530–3538.
[14] C.M. Herzinger, B. Johs, W.A. McGahan, J.A. Woollam, W. Paulson, Ellipsometric determination of optical constants for silicon and thermally grown silicon dioxide via a multi-sample, multi-wavelength, multi-angle investigation, J. Appl. Phys. 83 (1998) 3323–3336.
[15] A.G. Frutos, S.C. Weibel, R.M. Corn, Near infrared surface plasmon resonance measurements of ultrathin films. Part 1. Angle shift and SPR imaging experiments, Anal. Chem. 71 (1999) 3928–3934.